



Special Issue – 8th International Conference on Mechanical and Industrial Engineering, October 24 – 25, 2024 at The Nelson Mandela African Institute of Science and Technology, Arusha - Tanzania

Mitigation of Voltage Disturbances in Industrial Power Distribution Networks Using Dynamic Voltage Restorers

Godwin E. Mnkeni^{1,2}, Jackson J. Justo¹, Aviti T. Mushi^{1†} and Bakari M. M. Mwinyiwiwa¹

¹Department of Electrical Engineering, College of Engineering and Technology, University of Dar es Salaam, P.O. Box 35131, Dar es Salaam, Tanzania

²Department of Electrical and Power Engineering, Mbeya University of Science and Technology, P.O. Box 131, Mbeya, Tanzania

†Corresponding Author: aviti.thadei@udsm.ac.tz; ORCID: 0000-0002-2958-2919

ABSTRACT

Most electrical and electronic equipment in industries require high-quality power to function efficiently. Nonetheless, voltage sags and swells are pressing concerns and prone to directly impact the economy of industrial customers. One such customer embattled with these problems is Mbeya Cement Company Limited (MCC) located in Mbeya, Tanzania. These issues mainly are caused by upstream faults and switching operations. One way to address these is by utilizing the voltage injection method, which employs a power device known as a dynamic voltage restorer (DVR). In this paper, the voltage sags and swells of balanced three-phase, unbalanced double-line and single-line to ground faults are studied. Thereafter, mitigation strategies using the DVR are proposed for the MCC. A section of the MCC power distribution network fed from Tanzania Electric Supply Company Limited (TANESCO) Mwakibete substation with a 33 kV feeder is modeled using MATLAB/Simulink environment to mitigate the disturbances (sags/swells). The percentage of voltage sags and swells logged from the industrial feeder are 11 and 115%, respectively. To effectively utilize the DVR device, a control strategy is designed in the $d-q-o$ reference frame, whereby the scaled errors between the source side of the DVR and its references for sags/swells corrections are considered. Simulation results revealed that the DVR performance handles both balanced and unbalanced voltage sags and swells by injecting the appropriate voltage to the supply, therefore, maintaining the load voltage at its nominal value. It can be concluded that the DVRs are recommended to be incorporated into the MCC feeders to mitigate the upstream disturbances. However, DVR performance comes at the cost of energy storage and DVR transformer rating. Further studies are encouraged to focus on the DVR performance optimization and cost implications.

ARTICLE INFO

1st Submitted: **Apr. 23, 2024**

Presented: **Oct. 24, 2024**

Revised: **Nov. 26, 2024**

Accepted: **Jan. 30, 2025**

Published: **June, 2025**

Keywords: Dynamic voltage restorer, Voltage disturbances, Voltage sags, Voltage swells

INTRODUCTION

Electricity is a central part of modern society and a cornerstone of global socio-

economic development (Salite *et. al.*, 2021), powering a wide range of daily activities and technologies, while also improving productivity, comfort, safety,

health, and the economy (Bhonde *et. al.*, 2018; IEA, 2022). The Sustainable Development Goal (SDG) 7 insists on access to reliable electricity (IEA, 2022). In industries, reliable electricity is essential to avoid direct negative economic impact due to plant outages caused by unintentional trips of electrical protection systems. The electric power system that links industries is a vast network with generators, transmission lines, distribution lines, service lines, and consumer loads (Chawda *et. al.*, 2020). To achieve adequate power quality, all the network parameters must be managed so that they remain within acceptable voltage ranges. Power quality (PQ) in today's power distribution networks (PDN) is a crucial concern due to the widespread influx of sensitive electrical equipment and nonlinear loads present in industries (Abas *et. al.*, 2020; Mhagama *et. al.*, 2021; Tu *et. al.*, 2019). This means that the proliferation of sophisticated sensitive equipment whose performance is strongly dependent on supply quality has made power quality a prominent topic of concern in this era (Abas *et. al.*, 2020).

A power quality issue is when a nonstandard voltage, current, or frequency occurs, causing end-user equipment to fail or malfunction (Hossain *et. al.*, 2018). PQ can be distinguished based on the cause between disturbances related to the quality of supply voltage and those related to the quality of current taken by the load. Voltage quality problems appear as transients, sags, swells, flickers, and voltage imbalances, impairing the operation of industrial equipment with substantial economic losses (Awad *et. al.*, 2004; De Almeida Carlos *et. al.*, 2018). To address these PQ concerns, in PDN, three types of compensating custom power devices are widely used – dynamic voltage restorer (DVR), Distribution Static Compensator (DSTATCOM), and unified power quality conditioner (UPQC). These compensating custom power devices are designed and installed at the consumer side to meet acceptable voltage characteristics specified

by international standards such as (IEEE Std 1159, 2019; 2018). Among all the prominent compensating custom power devices, the literature suggests that DVR is the most technologically advanced and cost-effective device for mitigating voltage swells and sags, with the added benefit of active or reactive power control (Jayaprakash *et. al.*, 2014). The DVR is claimed to offer a rapid dynamic and economical approach to adjusting voltage disturbances, making it a high-performance solution for upstream fault prevention (Pal & Gupta, 2020). DVRs can adjust for the proper magnitude and phase angle of the source voltage, eliminating the bulk of voltage sags/swells, and they can handle voltage harmonic aberrations at the load terminals (Biricik *et. al.*, 2019; Shah *et. al.*, 2024).

Efforts have been devoted to studying the performance of DVR in mitigating load disturbances. Hakimzadeh & Sedaghati (2013) designed the DVR to mitigate single, and double-line-to-ground faults in a 230 kV, 50 Hz transmission line. The DVR used a pulse width modulation (PWM) control system, and its performance was evaluated using the PSCAD/EMTDC program. Salimin & Rahim (2011) designed a DVR with a proportional-integral (PI) and fuzzy logic controllers to mitigate voltage sags in an 11 kV distribution line. The model was tested against three-phase and double-line-to-ground faults using MATLAB/Simulink software. Soomro *et. al.* (2020) modeled a DVR with a PI controller to an 11 kV distribution line using MATLAB/Simulink to mitigate voltage sags that emerged in the form of harmonics. Sesay *et al.* (2014) employed a DVR with a fuzzy-based control scheme in a 33/0.4 kV distribution line to prevent voltage sags (which were 75%). The model was implemented on MATLAB/Simulink and simulated the three-phase and double-line-to-ground faults. Their findings revealed that the DVR compensated for the sags and swells rapidly and offered better (38.9%

improvement) voltage regulation. Gayatri et. al. (2016) employed a DVR with a $d-q-o$ scheme in a solar-wind-based microgrid to mitigate voltage sag and swell by using MATLAB/Simulink software, for which the voltage sag of 74% and swell of 127% of the nominal values were observed. With the application of DVR, the voltage disturbances were reduced and the voltages were restored to the nominal values.

Francis & Thomas (2014) adopted the $d-q-o$ technique to a DVR to compensate for the voltage sags (of 50%) and swells (of 50%) during a single-line-to-ground fault and three-phase-to-ground faults. The application of a DVR managed to reduce the sags and swells such that voltage was restored to the nominal values during faults. Kantaria et. al. (2010) adopted a $d-q-o$ algorithm to a DVR to mitigate the voltage sags and swells. Fanifosi et al. (2022) designed a DVR with a PI and $d-q-o$ technique to mitigate voltage sags in a 33 kV distribution line. The model was tested against three-phase and double-line-to-ground faults using MATLAB/Simulink software.

All these discussed previous studies have focused on mitigating voltage sags and swells present in the low-voltage and medium-voltage distribution lines. Nonetheless, the issues of disturbances found in industrial feeders are rarely adequately addressed. For example, the magnitudes and intervals of sags/swells disturbance modeled in the bulk of the cited research do not correspond to real-world industrial disturbances.

Therefore, this study models the DVR with the $d-q-o$ control technique to mitigate the voltage sags/swells disturbances emerging in the industrial feeders of Mbeya Cement Company (MCC) Limited.

METHODS AND MATERIALS

In the first part, the study logged the MCC feeder with NRS 048-2:2003 to assess the real-world voltage sags/swells industrial disturbances. The second part, models the MCC feeder and the DVR. The recorded

features of the voltage sags/swells disturbances are then incorporated into the study to understand the effectiveness of the modeled DVR. The findings of this study will pave the way toward designing a finite DVR, based on the recorded background real-world voltage sags/swells disturbances assessment, thus protecting the sensitive loads in that industry.

System Description of MCC Power Distribution Networks

Figure 1 depicts the MCC power distribution networks coming from TANESCO Mwakibete substation 33 kV feeder. At MCC two transformers of 6.3 MVA, 33/6.3 kV each are used to power 11 distribution feeder transformers of 6.3/0.4 kV. Despite being supplied by TANESCO with a 33 kV dedicated feeder, MCC has observed substantial voltage-related issues such as voltage sags and/or swells. To capture the sags and swells phenomena at MCC, the power was logged with NRS 048-2:2003 sag/swell assessment instrument for two weeks of June 2024 and 12 months of 2020.

Figures 2a and 2b indicate the proportion of exhibited sags and swells at MCC terminal voltage during those periods. The NRS 048 – 2 is a South African National Standard that deals with voltage sags/dips classifications based on their characteristics, compatibility levels, limits and assessment methods (NRS048, 2003). The NRS 048 – 2 standard categorizes voltage dips as types Y, S, X (X_1 and X_2), T, and Z (Z_1 and Z_2). These are explained as follows.

Type Y is a very fast decay sag, typically characterized by a rapid voltage reduction often in a few milliseconds. It is a short duration sag usually less than 10 milliseconds and has high repetitive rate often multiple times per second. Sags type Y are caused by faults in the power system, such as faults in the transmission or distribution networks or even faults within the customer premises. These fast and repetitive sags can be problematic to

sensitive equipment such as power electronic devices, motor drives or even renewable energy systems. Type S is a slow voltage dip/sag characterized by a gradual decrease in voltage magnitude, typically with duration more than 1 minute. Type S

sags are often caused by overload or faults in the distribution system. The slow nature of these sags can affect equipment that relies on stable voltage supply such as motor drives or power electronic devices.

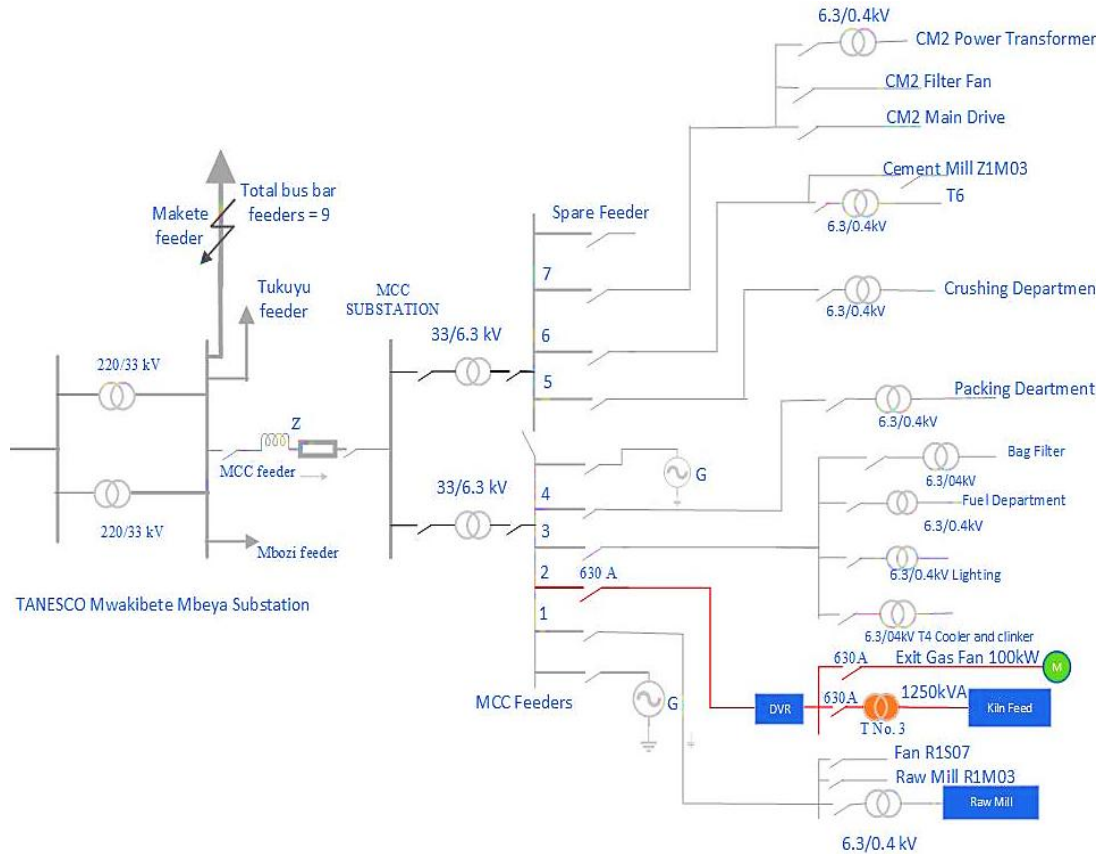
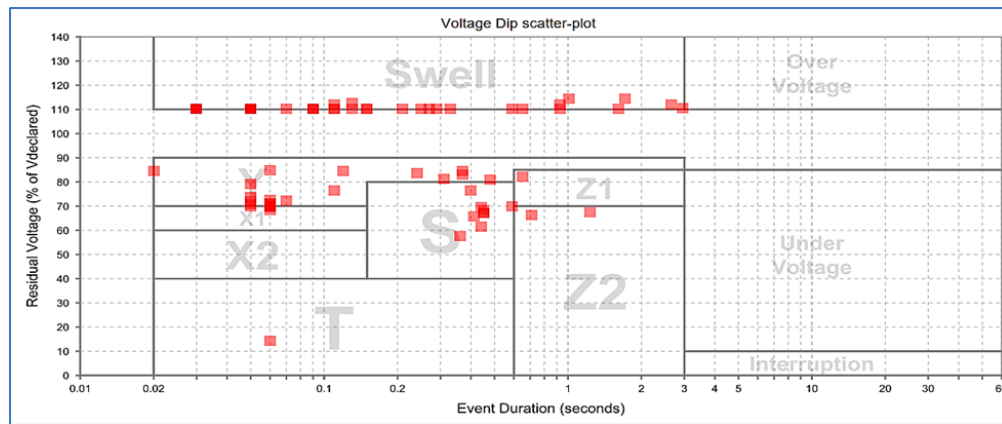


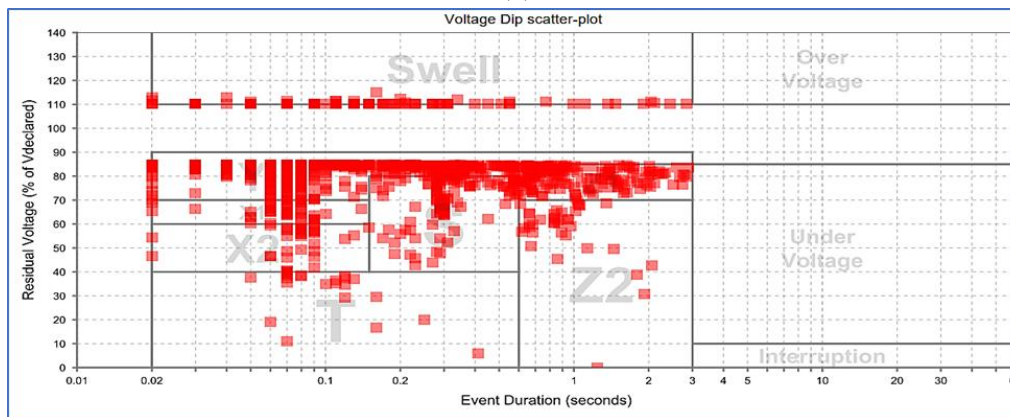
Figure 1: MCC power distribution networks.

Type X_1 and X_2 are both classified as type X, known as interruptible sags. These are intentional voltage reductions, usually lasting from a few seconds to several minutes, implemented by power utilities to balance load and generation during peak demand periods or when performing maintenance. The main distinction of these sags lies in the duration and frequency of occurrence. Type X_1 are short duration typically lasting less than one second and occurring infrequently while type X_2 sags are longer duration typically lasting between one second and three minutes occurring more frequently. Type T are transient sags, characterized by rapid voltage reduction between 12% and 40% of the nominal value typically lasting less than

one minute, and often caused by faults in the power system. This type of voltage sag is considered a moderate severity sag and its classification is important for the design and operation of an electrical system. Type Z is defined as voltage sag with a complex waveform which can be irregular or oscillatory, often featuring multiple consecutive voltage reductions with varying depths and durations. The main distinction between Z_1 and Z_2 lies in the repetition rate and duration of the individual sag event within the complex waveform. Type Z_1 sag tend to be more frequent and shorter, while type Z_2 are less frequent and longer.



(a)



(b)

Figure 2: Event sags and swells recorded by NRS 048-2:2003 (a) 20% displayed for two weeks of June 2024; and (b) 1.6% displayed event for 12 months January – December 2020.

As indicated in Figure 2, the MCC power distribution network is highly affected by upstream faults that occur on the transmission line. These faults cause sudden drop or increase in voltage proliferations. Figure 2a, displays 20% recorded events of the sags and swells for two weeks of June 2024, with typical residual voltage between 14 and 85%. In terms of swell, the typical residual voltage ranges between 110 and 115%. Figure 2b, shows 1.6% recorded voltage sags events measured for the reported 12 months of 2020, with typical residual voltage between 11 and 88%. In the case of the swells, the typical residual voltage is around 112%. Majority of events are due to voltage sags (approximately 90%). These in turn affect MCC operations leading to inefficiencies, downtime, damaged equipment, and captive power costs.

This study proposes designing and installing DVRs in all seven MCC distribution feeders to ensure that MCC-sensitive loads receive the necessary voltage quality, thus improving system stability and reliability.

Reference Power Distribution Network

Figure 1 shows the radial distribution network of the MCC. Its power source is the TANESCO Mwakibete substation switch yard feeding two 33/6.3 kV, 6.3 MVA step-down transformers. The reference power distribution network of MCC is Feeder 2, used to simulate the sags and swells phenomena. The sags and swells simulations are performed under three conditions which are: – the normal condition, fault condition, and mitigation condition. The reference feeder was simulated in two cases which are using a three-phase (3 ϕ) balanced main supply and

using three-phase two-lines and single-line (1Ø) unbalanced voltage supply. The voltage unbalance caused by the unbalanced upstream faults were adopted from the actual reference feeder's recorded deviations shown in Figure 2. Based on Figure 2, the severity voltage sag and swell of 11 and 115% were taken into consideration.

Mathematical Modelling of Distribution Network with DVR

The distribution transformers at MCC (Figure 1), are connected in delta-star type, therefore zero-sequence currents on the delta side are blocked from passing to the star side. Hence, only restoration of positive sequence and negative sequence voltage is required (Bhonde et al., 2018). The winding configuration of the injection transformer depends mainly on the upstream distribution transformer (Pal & Gupta, 2020). For this case, open-delta injection transformer (Figure 3) is proposed with the advantages of maximizing the utilization of DC link voltage (Li et al., 2007; Zhan et al., 2001). The DVR system has two major parts, the power circuit and the control circuit. The power circuit consists of an injection transformer, a voltage source converter, energy storage, and passive filters. The series injection transformer serves as a conjunction device between the DVR and the PDN, thus understanding the dimensions and characteristics of the PDN is essential for its design. This determines the voltage source inverter (VSI) ratings, DC capacitor ratings, ride-through capabilities, compensator ability, and dependability (Sasitharan et al., 2008). The characteristics to be determined for DVR system power circuit design are the following:

- (i) The power (MVA) rating of the critical load to be protected,
- (ii) The maximum acceptable voltage drops across the injection transformer,
- (iii) The severity of the sags/swells in magnitude to be compensated,

- (iv) The design of the harmonic filter system,
- (v) The selection of the switching devices, and
- (vi) The energy storage capacity and the voltage restoration control strategy.

The single-line diagrams of the reference MCC distribution network are shown in Figures 4 and 5. The DVR is used to mitigate the supply voltage disturbances by injecting voltage in series with the line to achieve disruption-free supply at the load terminals. The series converter in Figures 4 and 5, can be represented by the Equations (1) – (6),

$$V_{DVR}(\omega t) = V_L(\omega t) - V_t(\omega t) \quad (1)$$

where $V_{DVR}(\omega t)$, $V_L(\omega t)$, and $V_t(\omega t)$ represent the converter injected voltage, loads voltage, and the distorted supply voltage at the point of common coupling respectively. The power rating of the DVR can be calculated as follows.

$$S_i + S_{DVR} = S_L \quad (2)$$

$$S_{DVR} = S_L - S_t = (S_1 + S_2) - S_t \quad (3)$$

Assume the loads at normal operation are supplied at load power factor 0.9 lagging. Therefore,

$$V_L(\omega t) I_{L<\theta} = \frac{1}{\sqrt{3}} (S_1 + \frac{P_1}{0.9}). \quad (4)$$

$I_{L<\theta}$ is the series current of the feeder passing through the DVR, hence its rating is given by Equation (5).

$$S_{DVR} = \sqrt{3} I_{L<\theta} V_{DVR} \quad (5)$$

The DVR model is depicted as an inverter with an LCL harmonic filter where the inductance of the injection transformer is taken into consideration. Neglecting the higher order harmonics, the VSI can be represented as an ideal AC source (V_{inv}), in Figure 5 (Equation (6)).

$$V_{DVR} = V_{inv} - I_{L<\theta} Z_{eq} \quad (6)$$

The Equation (1) indicates that the load voltage depends on the supply voltage at PCC and the injected voltage V_{DVR} . Equation (6) shows that the restoration process must include the restoration of the voltage drop within the DVR internal impedance. Injection transformer design is a very crucial element in DVR as the

transformer may reach saturation, overrating, and overheating issues (Sasitharan et al., 2008).

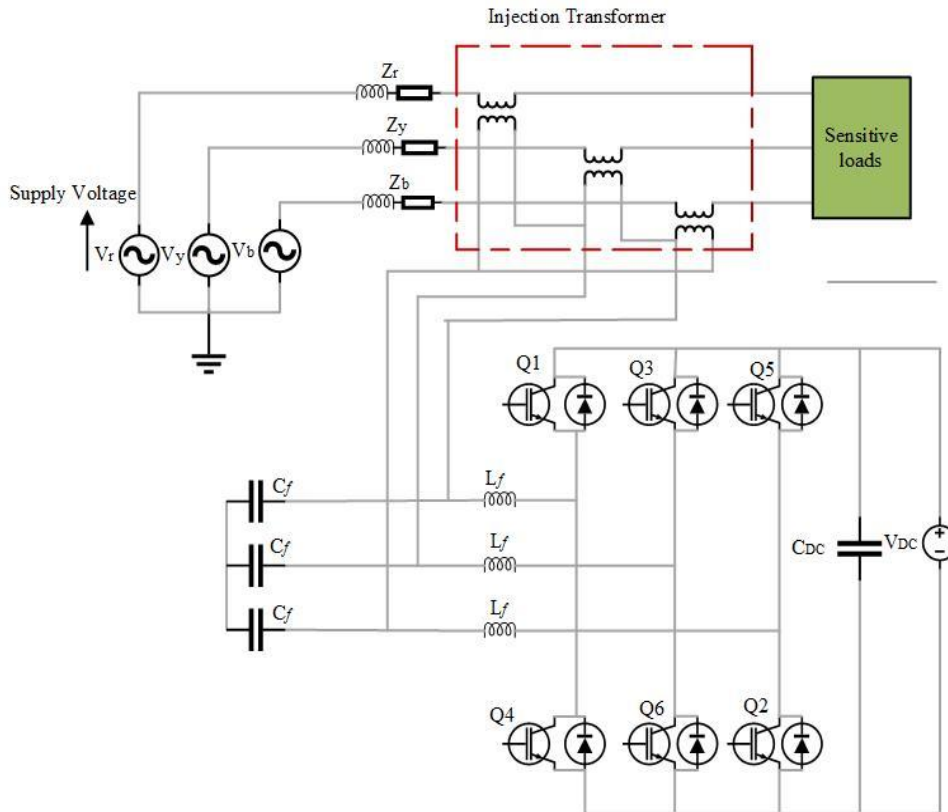


Figure 3: The proposed circuit of DVR at MCC feeder 2.

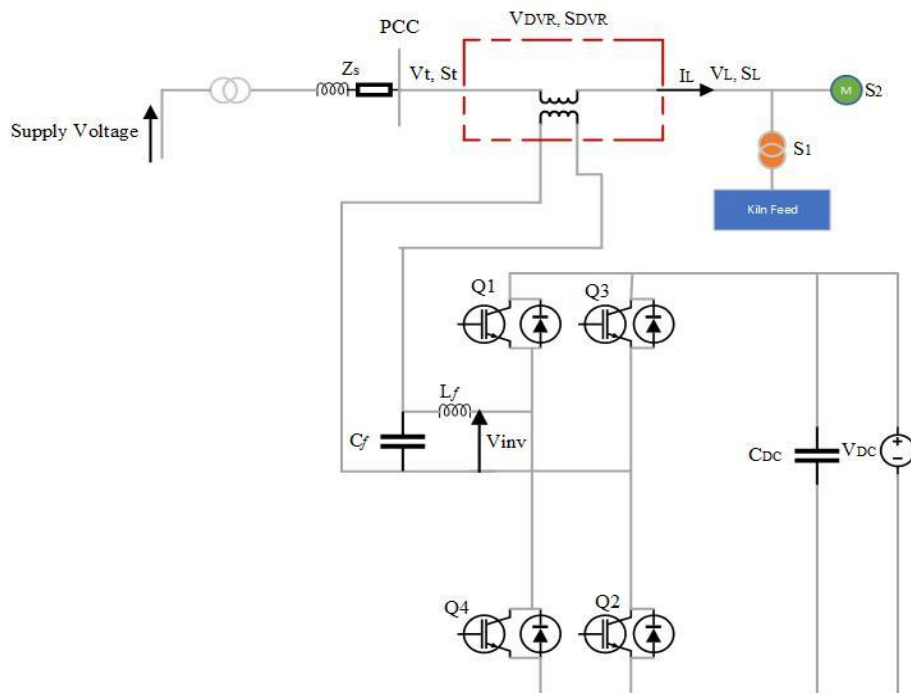


Figure 4: The single-line representation of MCC feeder 2.

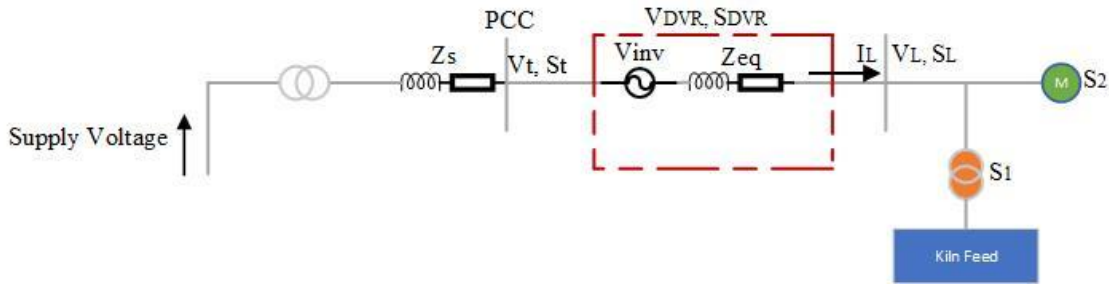


Figure 5: The simplified single-line representation of MCC feeder 2.

A parameter that influences the rating of the DVR is the severity/maximum single-phase and three-phase voltage sag/swell to be compensated (Equation (7)), named V_{sag} .

$$V_{sag} (\%) = \left(1 - \frac{V_{sag}}{V_{nominal}}\right) \times 100 \quad (7)$$

The primary function of the harmonic filter is to maintain the allowable level of harmonic voltage content produced by the VSI. The filter is positioned to reduce the switching harmonics produced by the VSI's PWM control. Determination of the harmonic filter parameters involves determining the cut-off frequency f_c of the filter chosen to be lower than the switching frequency f_s of the inverter but higher than the fundamental frequency f_o of the system, see Equation (8).

$$f_c = \frac{1}{2\pi\sqrt{L_f C_f}} \quad (8)$$

The value of the inductance L_f is chosen based on the desired current ripple. A typical range for the inductance is calculated using Equation (9).

$$L_f = \frac{V_{dc}}{4\Delta I f_s} \quad (9)$$

Where V_{dc} is the DC link voltage, ΔI is the allowable current ripple. The value of the capacitance C_f is calculated based on the desired cut-off frequency f_c by Equation (10).

$$C_f = \frac{1}{(2\pi f_c)^2 L_f} \quad (10)$$

During the voltage sag these energy storage devices deliver the required real power. The DC-link voltage (V_{dc}) is approximately equal to the peak phase-phase value of the supply voltage, and the energy stored E is

proportional to the square of the rated DC-link voltage.

$$E = \frac{1}{2} C_{dc} V_{dc}^2 \quad (11)$$

During sag compensation the allowable change in voltage is given by Equation (12).

$$3V_{inj} \times i_L \times \Delta t = \frac{1}{2} C_{dc} \times (V_{dc}^2 - \Delta V_{dc}^2) = \Delta E \quad (12)$$

The rating of the DC-bus capacitor C_{dc} is shown by Equations (13) – (14).

$$C_{dc} = \frac{6V_{inj} \times i_L \times \Delta t}{(V_{dc}^2 - \Delta V_{dc}^2)} \quad (13)$$

$$V_{dc} \geq 2\sqrt{2} \times (V_{inj}) \quad (14)$$

Where V_{inj} is the injection transformer's primary winding voltage. For the MCC case, the injection transformer is assumed ideal with a turn's ratio of 1:1. Also the injected voltage by the DVR is adopted after taking into account the voltage drop across the harmonic filter system. The VSI voltage rating is selected to ensure that it can provide the injection transformer with sufficient voltage, and the current rating is selected to match the load current. Neglecting the interruptions, from Equation (7) the severity sag at MCC for these two logged power data of 2020 and 2024 was 11.1% equal to 5.607 kV (line voltage). Equations (1) to 14) are used to compute the required DVR parameters, which are indicated in Table 1.

Table 1: Specifications of the DVR parameters

Parameters	Unit	Value
Grid line voltage	kV	6.3
DVR control voltage	V	400
Load power rating	kVA	1,361.11

Parameters	Unit	Value
DVR power rating	kVA	1,214.20
DVR voltage rating	V	3,238
DVR current rating	A	216.50
Voltage source converter (VSC)		IGBT/diode, 3 arms 6 pulses 3.3 kV, $f_s = 10$ kHz
RC filter inductance	mH	1,000
RC filter capacitance	μ F	600
Injection transformer	V	1:1 (3,238 V: 3,238 V)
DC link voltage	kV	9.33

The Proposed DVR Control System Design

Figure 6 depicts the proposed DVR control system. The control system employs synchronous reference frame (SRF) and a pre-sag compensation strategy.

This strategy can restore the required voltage magnitude and the phase shift as upstream faults are associated with phase shifts. To regulate the VSC switching device, the DVR control system should perform the following functions:

- (i) Detect the supplied and the load voltage disruptions,
- (ii) Detect the supplied voltage angle for synchronization,
- (iii) Calculate the reference voltage and the compensation voltage value required, and
- (iv) Generate the required pulses for switching the VSC.

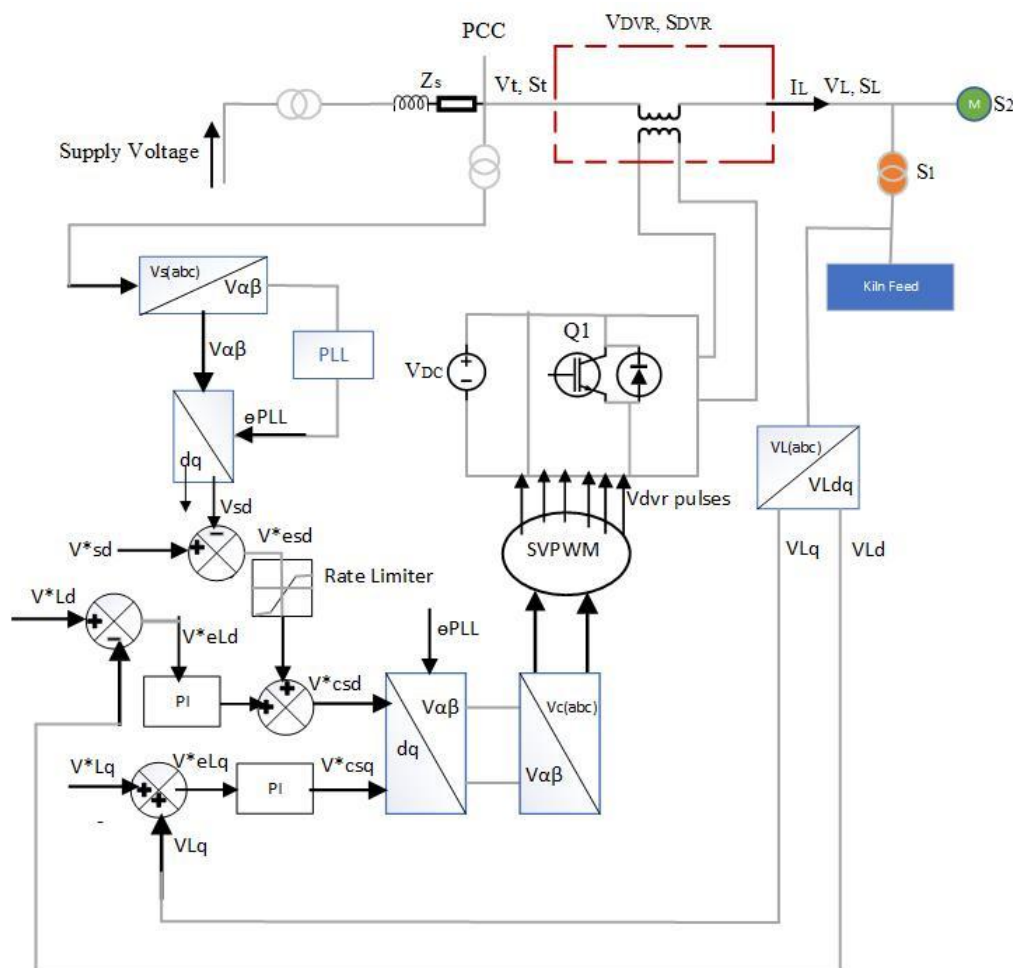


Figure 6: The proposed DVR control system.

The input voltages (V_{sa}, V_{sb}, V_{sc}) at the PCC, and the load voltages (V_{La}, V_{Lb}, V_{Lc}), are first transformed into the two-phase stationary coordinates

using the $\alpha\beta$ transformation by applying Park's transformation. The sine and cosine unit vectors ($\sin\theta$, $\cos\theta$), which are obtained from the widely used grid synchronization technique phase-locked loop (PLL), are then implemented and transferred into the synchronous reference frame d-q-0 (V_d and V_q). The sine and cosine unit vectors help to keep the source voltage vector angular position (θ) in sync with the supply voltage. The matrix expressions (15) - (23) represent the conversion of source voltages from the abc frame into the rotating synchronous reference d-q-0 frame via the abc-dq0 conversion. Where (V_{sa} , V_{sb} , and V_{sc}) are the RMS of the supply voltage (phase to neutral).

$$\begin{bmatrix} V_\alpha \\ V_\beta \\ V_0 \end{bmatrix} = A \begin{bmatrix} V_{sa} \\ V_{sb} \\ V_{sc} \end{bmatrix} \quad (15)$$

$$\begin{bmatrix} V_\alpha \\ V_\beta \\ V_0 \end{bmatrix} = V_m \sqrt{\frac{2}{3}} \begin{bmatrix} 1 & -\frac{1}{2} & -\frac{1}{2} \\ 0 & \frac{\sqrt{3}}{2} & -\frac{\sqrt{3}}{2} \\ \frac{1}{\sqrt{2}} & \frac{1}{\sqrt{2}} & \frac{1}{\sqrt{2}} \end{bmatrix} \begin{bmatrix} \cos \omega t \\ \cos \left(\omega t - \frac{2\pi}{3} \right) \\ \cos \left(\omega t + \frac{2\pi}{3} \right) \end{bmatrix} \quad (16)$$

$$\begin{bmatrix} V_{sd} \\ V_{sq} \end{bmatrix} = \begin{bmatrix} \cos \omega t & \sin \omega t \\ -\sin \omega t & \cos \omega t \end{bmatrix} \begin{bmatrix} V_\alpha \\ V_\beta \end{bmatrix} \quad (17)$$

Where $V_m = \sqrt{2}V_s$ is the peak phase value. Similarly, the actual and reference load voltages (V_{La} , V_{Lb} , and V_{Lc}) are transformed to get the V_{Ld} , and V_{Lq} components through Equation (18).

$$\begin{bmatrix} V_{Ld} \\ V_{Lq} \end{bmatrix} = \begin{bmatrix} \cos \omega t & \sin \omega t \\ -\sin \omega t & \cos \omega t \end{bmatrix} \begin{bmatrix} V_{La} \\ V_{Lb} \end{bmatrix} \quad (18)$$

Then, the supply voltage scaled error of the DVR voltages are obtained in the rotating reference frame as per Equations (19) – (20).

$$V_{esd}^* = V_{sd}^* - V_{Ld} \quad (19)$$

$$V_{esq}^* = V_{sq}^* - V_{Lq} \quad (20)$$

The reference DVR scaled error load voltages are obtained in the rotating reference frame as per Equations (21) and

(22).

$$V_{eLd}^* = V_{Ld}^* - V_{Ld} \quad (21)$$

$$V_{eLq}^* = V_{Lq}^* - V_{Lq} \quad (22)$$

The error between the reference and actual DVR voltages obtained in the rotating reference frame are regulated using two proportional-integral controllers. The reference DVR voltage in abc frame is obtained from the Reverse Park's Transformation taking V_{cd}^* and V_{cq}^* from Equation (23), while setting V_{c0}^* as zero.

$$\begin{bmatrix} V_{dvra} \\ V_{dvrb} \\ V_{dvrc} \end{bmatrix} = \sqrt{\frac{2}{3}} \begin{bmatrix} 1 & 0 & \frac{1}{\sqrt{2}} \\ -\frac{1}{2} & \frac{\sqrt{3}}{2} & \frac{1}{\sqrt{2}} \\ -\frac{1}{2} & -\frac{\sqrt{3}}{2} & \frac{1}{\sqrt{2}} \end{bmatrix} \begin{bmatrix} V_\alpha \\ V_\beta \\ V_0 \end{bmatrix} \quad (23)$$

The output is a vectorized signal containing three (V_{dvra} , V_{dvrb} , V_{dvrc}) phase sinusoidal quantities used in the PWM controller to generate gating pulses to the VSC of the DVR. The PWM controller at MCC is operated with a switching frequency of 10 kHz.

RESULTS AND DISCUSSIONS

Simulation of voltage sags and swells disturbances on the MCC Feeder 2 was done by generating faults using a 3-phase fault generator at a feeder connected parallel to MCC feeder until the sag phenomenon was observed. DVR was inserted into the MCC Feeder 2 to restore the feeder voltage. Three types of faults were generated at the supply side to produce the sagging phenomenon which is a balanced three-phase fault; single-phase-to-ground fault and double-line-to-ground fault (unbalanced). The total simulation time was 0.5 seconds while the sagging and swelling phenomena were targeted to trigger between 0.15 and 0.35 seconds. In both fault conditions, the performance of the DVR is analyzed to investigate how efficiently it can mitigate voltage sags and swells disturbances.

Voltage Sags

Figure 7 shows the results of voltage sags for the balanced fault (three-phase). As shown in Figure 7(a), the first simulation of three-phase voltage sag is simulated when 11% of three-phase voltage sag occurs at the MCC Feeder 2. It can further be shown that voltage sag is initiated at 0.15 seconds and it is kept until 0.35 seconds, with a total voltage sag duration of 0.2 seconds. Figure 7(b) shows the injected three-phase voltage from the DVR to MCC feeder 2. The voltage injected by the DVR and the corresponding load voltage with compensation is shown in Figure 7(c). After compensation from the DVR, the load voltage is kept at 1 pu as shown in Figure 7(c).

Figures 8 and 9 show the results of voltage sag for the unbalanced faults (double-line and single-line to ground fault). As shown in Figure 8(a), the simulation of two-line voltage sag is simulated when 11% of two-phase voltage sag occurs at the MCC Feeder 2. It can be shown that a voltage sag is triggered for 0.2 seconds (from 0.15 seconds to 0.35 seconds). The DVR injected voltage and load voltage are shown in Figures 8(b) and (c).

Figure 9 shows the simulation of single-phase voltage for the unbalanced fault. The sag simulates 11% of the single-phase voltage sag occurring at the MCC Feeder 2.

The voltage injected by the DVR and the corresponding load voltage with compensation is shown in Figure 9(b) and (c). After compensation from the DVR, the load voltages in both two-line and single-line (Figures 8(c) and 9(c)) are kept at 1 pu. In these cases of balanced and unbalanced voltage sags, the DVR reacts quickly to inject the appropriate amount of positive voltage component to correct the supply voltage.

Figures 10 and 11 show the results of voltage swell for the balanced and unbalanced three-phase faults. In both Figures 10 and 11, the amplitude of the supply voltage was raised by about 15% of its working voltage. This means that the swell was simulated by 115% of the working voltage. The 115% was adopted from the most common swell faults as recorded in the MCC Feeders (previously shown by Figure 2).

For the balanced three-phase fault, shown in Figure 10(a), the supply voltage swell is triggered for a duration of 0.2 seconds (from 0.15 seconds to 0.35 seconds). Figure 10(b) shows the absorbed swells voltage by the DVR from the disturbed supply voltage. It can be seen that the load voltage is kept at the nominal value after integrating the DVR voltage compensation.

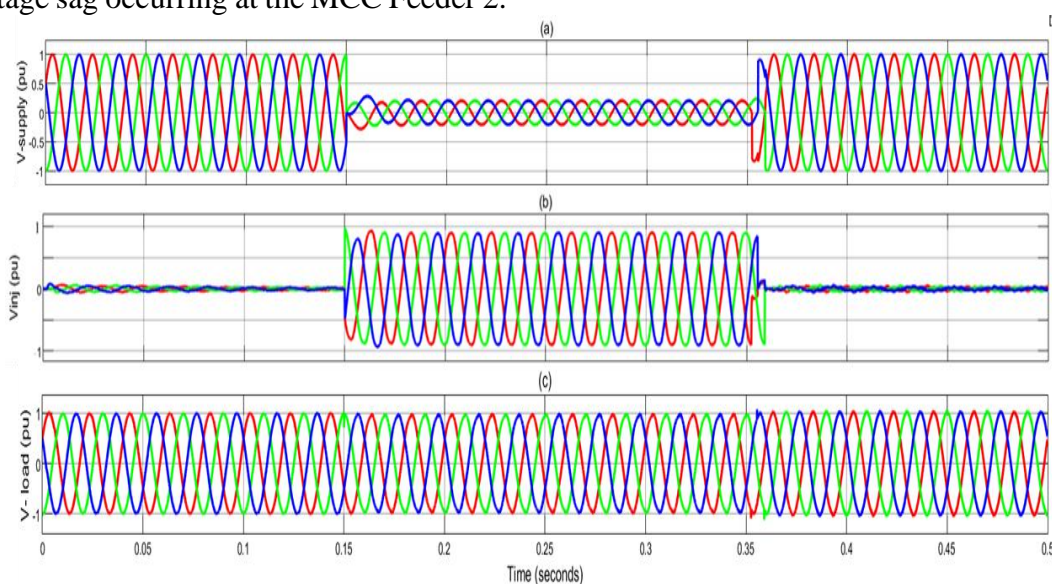


Figure 7: Three-phase balanced sag of 11% of the source voltage waveform (p.u.) (a) under sag disturbances; (b) DVR injected voltage; and (c) compensated load voltage waveform.

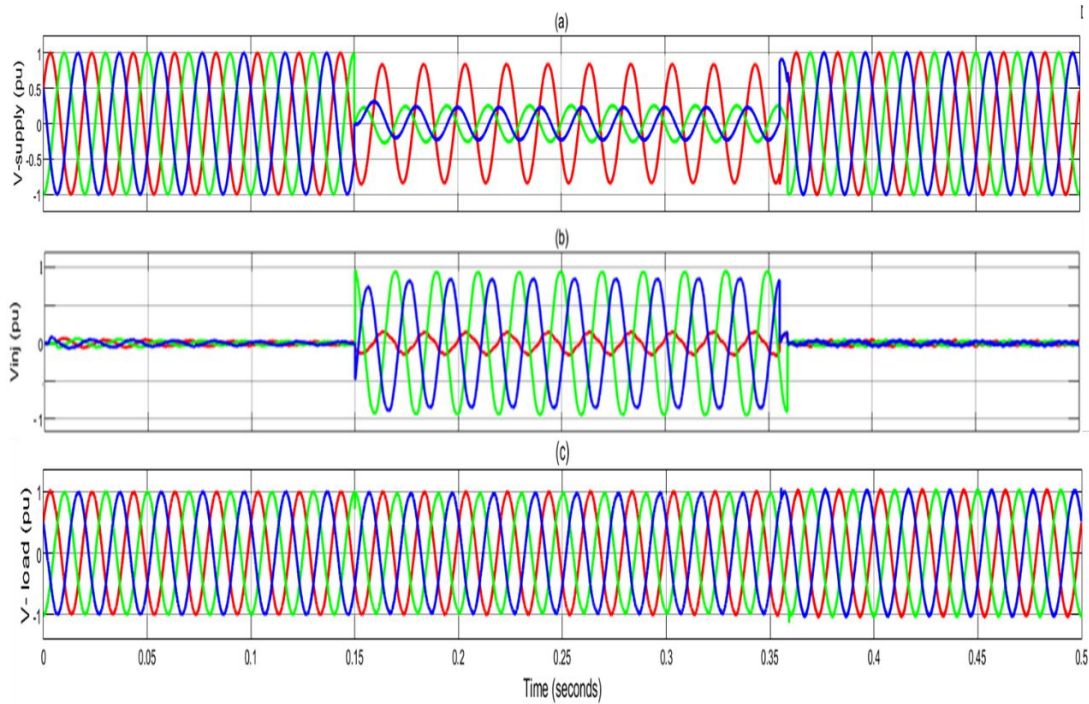


Figure 8: Double-line unbalanced sag of 11% of the supply voltage waveform in (p.u.) (a) under sag disturbances; (b) DVR injected voltage; and (c) compensated load voltage waveform.

Voltage Swell

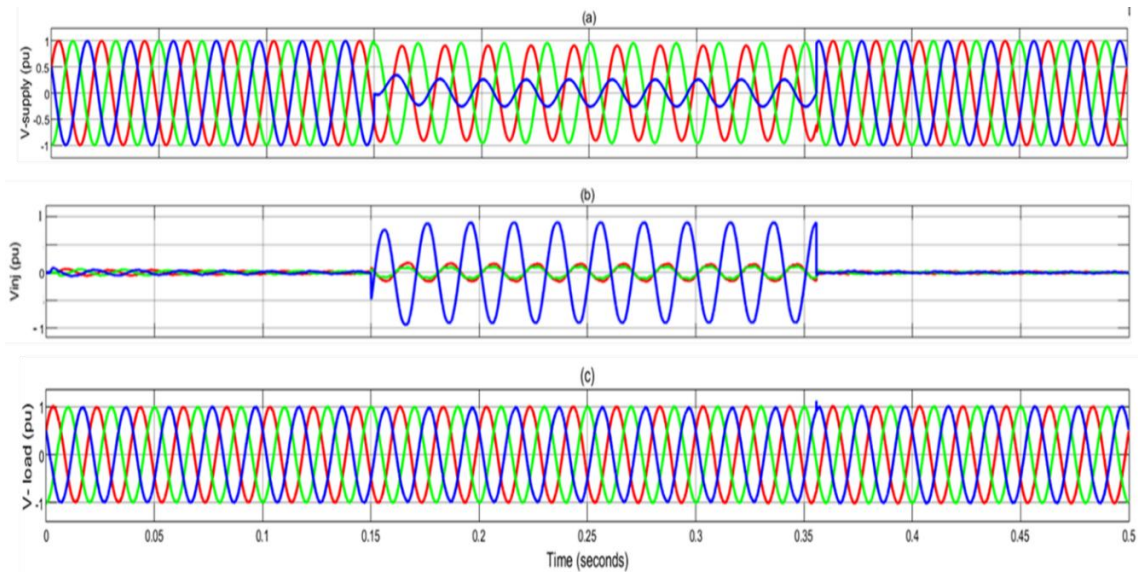


Figure 9: Single-line unbalanced sag of 11% of the supply voltage waveform in (p.u.) (a) under sag disturbances; (b) DVR injected voltage; and (c) compensated load voltage.

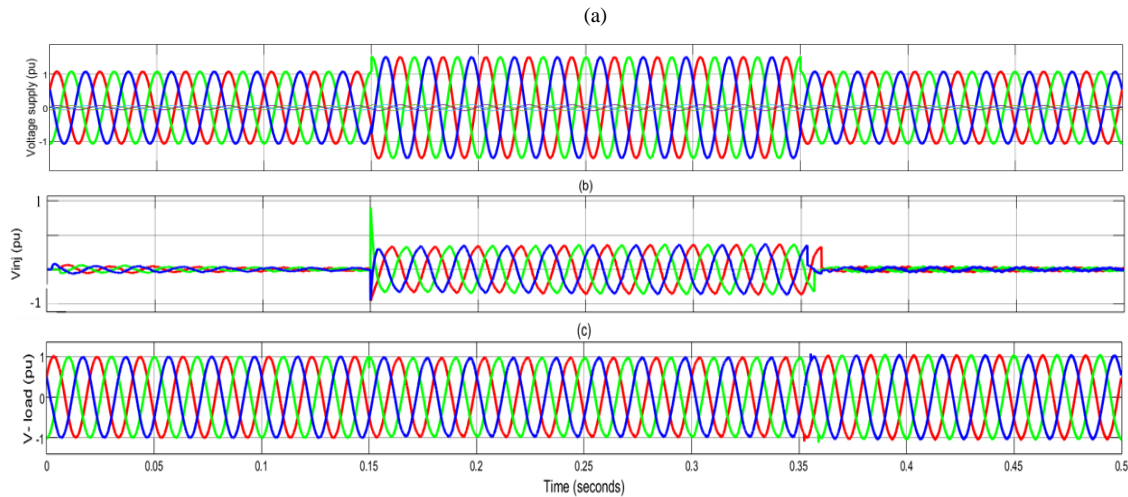


Figure 10: Three-phase balanced voltage swell fault (a) a 15% increase in supply voltage; (b) DVR absorbed voltage swells; and (c) voltage waveforms at load after compensation.

In comparison to the case of voltage swell presented in Figure 10, Figure 11 simulates an increase of 15% of unbalanced three-phase working voltage. For the unbalanced three-phase fault, shown in Figure 11(a), the supply voltage swell is triggered for a duration of 0.2 seconds (from 0.15 seconds to 0.35 seconds). Figure 11(b) shows the absorbed swells voltage by the DVR from

the unbalanced three-phase working voltage. It can be seen that the load voltage is kept at the nominal value after incorporating the voltage from the DVR. In this case of voltage swell, the DVR reacts quickly to inject the appropriate amount of negative voltage component to correct the supply voltage swells.

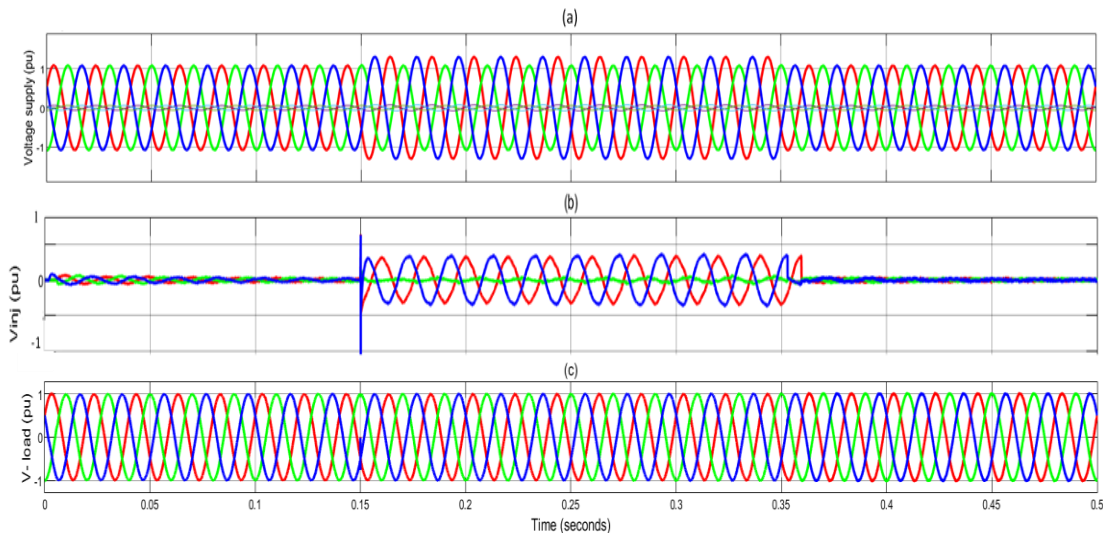


Figure 11: Three-phase unbalanced voltage swell fault (a) a 15% increase in supply voltage; (b) DVR absorbed voltage swells; and (c) voltage waveforms at load after integrating negative voltage component from the DVR.

Table 2: Performance Comparative analysis per phase voltage

Author	Scenario % residual voltage	Nominal voltage, V_N	Voltage change/	Compensated amount,
--------	--------------------------------	---------------------------	--------------------	------------------------

			residual voltage ΔV	$\Delta V_C = V_{DVR} = V_{sag}/V_{swell}$
Francis & Thomas (2014)	Voltage sag, $\Delta V = 50\%$	239.6 V	119.8 V	+119.8V
	Voltage swell, $\Delta V = 150\%$	239.6 V	119.8 V	-119.8V
Kantaria <i>et. al.</i> (2010)	Voltage sag, $\Delta V = 40\%$	100 V	60 V	40 V
	Voltage swell, $\Delta V = 140\%$	100 V	140 V	-40 V
This paper	Voltage sag, $\Delta V = 11\%$	3638 V	400.0 V	+3,238 V
	Voltage swell, $\Delta V = 115\%$	3638 V	4183.7 V	- 545.7 V

To summarize the performance analysis of the DVR installed on the industrial feeder, Table 2 shows the comparative results under voltage sag of 11% and swell of 115% residual voltage; compared to other previous literature.

CONCLUSION

This paper has proposed designing a finite DVR, based on the recorded background real-world voltage sags/swells disturbances assessment at MCC Limited power distribution network. The study logged the MCC feeder with NRS 048-2:2003 to assess the real-world voltage sags/swells industrial disturbances. The severity voltage sag and swell of 11 and 115% were recorded and used to design a finite DVR. A sectional part of the MCC Limited power distribution networks fed by TANESCO's Mwakibete substation with a 33 kV feeder was modeled using MATLAB/Simulink environment to mitigate the disturbance sags and/or swells at the terminal of the MCC loads. The performance of the reference feeder was investigated with and without the inclusion of that designed finite DVR when there were severe voltage disturbances (sags/swells). DVR control was based on the *d-q-o* technique which is a scaled error between the source side voltage of the DVR and its references for sags/swells corrections. It was revealed that the finite DVR handles both balanced and unbalanced voltage sags and swells by

injecting the appropriate voltage component to the supply voltage and maintaining the load voltage at its nominal value. The simulation shows that the finite DVR performance is satisfactory in mitigating voltage sags/swells. The DVRs are recommended to be incorporated into the MCC feeders to mitigate the upstream voltage disturbances, thus protecting the sensitive loads in the industry. However, this performance comes at the cost of an energy source at the DC bus and injection transformer rating. Further studies are encouraged to focus on the DVR performance optimization, cost implications, and wider comparison with existing literature.

Acknowledgement

This research was financially supported by the Mbeya University of Science and Technology under Ministry of Education Science and Technology HEET Project.

REFERENCES

- Abas, N., Dilshad, S., Khalid, A., Saleem, M. S., & Khan, N. (2020). Power quality improvement using dynamic voltage restorer. *IEEE Access*, 8, 164325–164339. doi:10.1109/ACCESS.2020.3022477
- Awad, H., Svensson, J., & Bollen, M. (2004). Mitigation of unbalanced voltage dips using static series compensator. *IEEE Transactions on Power Electronics*,

- 19(3), 837–846. doi:10.1109/TPEL.2004.826536
- Bhonde, S. V., Jadhao, S. S., & Pote, R. S. (2018). Enhancement of Voltage Quality in Power System through Series Compensation using DVR. *International Conference on Current Trends in Computer, Electrical, Electronics and Communication, CTCEEC 2017*, 826–830. doi:10.1109/CTCEEC.2017.8455101
- Biricik, S., Komurcugil, H., Tuyen, N. D., & Basu, M. (2019). Protection of sensitive loads using sliding mode controlled three-phase DVR with adaptive notch filter. *IEEE Transactions on Industrial Electronics*, 66(7), 5465–5475. doi:10.1109/TIE.2018.2868303
- Chawda, G. S., Shaik, A. G., Mahela, O. P., Padmanaban, S., & Holm-Nielsen, J. B. (2020). Comprehensive Review of Distributed FACTS Control Algorithms for Power Quality Enhancement in Utility Grid with Renewable Energy Penetration. *IEEE Access*, 8, 107614–107634. doi:10.1109/ACCESS.2020.3000931
- De Almeida Carlos, G. A., Jacobina, C. B., Mélló, J. P. R. A., & Dos Santos, E. C. (2018). Cascaded Open-End Winding Transformer Based DVR. *IEEE Transactions on Industry Applications*, 54(2), 1490–1501. doi:10.1109/TIA.2017.2768531
- Fanifosi, S., Ike, S., Buraimoh, E., & Davidson, I. E. (2022). 33kV Distribution Feeder Line Sag and Swell Mitigation using Customized DVR. *Proceedings of the 5th International Conference on Information Technology for Education and Development: Changing the Narratives Through Building a Secure Society with Disruptive Technologies, ITED 2022*, 14–18. doi:10.1109/ITED56637.2022.10051316
- Francis, D., & Thomas, T. (2014). Mitigation of voltage sag and swell using dynamic voltage restorer. *2014 Annual International Conference on Emerging Research Areas: Magnetics, Machines and Drives, AICERA/ICMMD 2014 - Proceedings*. doi:10.1109/AICERA.2014.6908218
- Gayatri, M. T., Parimi, A. M., & Kumar, A. (2016). Application of Dynamic Voltage Restorer in microgrid for voltage sag/swell mitigation. *2015 IEEE Power, Communication and Information Technology Conference, PCITC 2015 - Proceedings*, 750–755. doi:10.1109/PCITC.2015.7438096
- Gong, J., Li, D., Wang, T., Pan, W., & Ding, X. (2021). A comprehensive review of improving power quality using active power filters. *Electric Power Systems Research*, 199(June), 107389. doi:10.1016/j.epsr.2021.107389
- Hakimzadeh, M., & Sedaghati, R. (2013). Performance study of dynamic voltage restorer (DVR) in order to power quality improvement. *Advanced Materials Research*, 622, 1830–1834. doi:10.4028/www.scientific.net/AMR.622-623.1830
- Hossain, E., Tur, M. R., Padmanaban, S., Ay, S., & Khan, I. (2018). Analysis and Mitigation of Power Quality Issues in Distributed Generation Systems Using Custom Power Devices. *IEEE Access*, 6(c), 16816–16833. doi:10.1109/ACCESS.2018.2814981
- IEA. (2022). Tracking SDG 7: The Energy Progress Report. *Iea*, 158–177.
- IEEE Std 1159. (2019). IEEE Recommended Practice for Monitoring Electric Power Quality. In *IEEE Std 1159-2019 (Revision of IEEE Std 1159-2019)* (Vol. 2019, Issue 13 June).
- IEEE. (2018). IEEE Guide for Identifying and Improving Voltage Quality in Power Systems, in *IEEE Std 1250-2018 (Revision of IEEE Std 1250-2011)*: 1-63. doi:10.1109/IEEESTD.2018.8532376.
- Jayaprakash, P., Singh, B., Kothari, D. P., Chandra, A., & Al-Haddad, K. (2014). Control of reduced-rating dynamic voltage restorer with a battery energy storage system. *IEEE Transactions on Industry Applications*, 50(2), 1295–1303. doi:10.1109/TIA.2013.2272669
- Kantaria, R. A., Joshi, S. K., & Siddhapura, K. R. (2010). A novel technique for mitigation of voltage sag/swell by Dynamic Voltage Restorer (DVR). *2010 IEEE International Conference on Electro/Information Technology*,

- EIT2010, 2–5. doi:10.1109/EIT.2010.5612089
- Li, Y. W., Loh, P. C., Blaabjerg, F., & Vilathgamuwa, D. M. (2007). Investigation and improvement of transient response of DVR at medium voltage level. *IEEE Transactions on Industry Applications*, 43(5), 1309–1319. doi:10.1109/TIA.2007.904430
- Mhagama, G., Mushi, A.T., & Kundy, B.J. (2021). Performance Evaluation of DSTATCOM for 180 km 33 kV Feeder from Shinyanga to Bariadi in Tanzania. *Jordan Journal of Electrical Engineering (JJEE)*, 7(4): 344-359. doi:10.5455/jjee.204-204-1610344139
- NRS048. (2003). *Electricity Supply — Quality of Supply Part 2: Voltage characteristics, compatibility levels, limits and assessment methods*. Technology Standardization Department (TSD), Eskom.
- Pal, R., & Gupta, S. (2020). Topologies and Control Strategies Implicated in Dynamic Voltage Restorer (DVR) for Power Quality Improvement. *Iranian Journal of Science and Technology - Transactions of Electrical Engineering*, 44(2), 581–603. doi:10.1007/s40998-019-00287-3
- Salimin, R. H., & Rahim, M. (2011). Simulation analysis of DVR performance for voltage sag mitigation. *2011 5th International Power Engineering and Optimization Conference, PEOCO 2011 - Program and Abstracts, June*, 261–266. doi:10.1109/PEOCO.2011.5970386
- Salite, D., Kirshner, J., Cotton, M., Howe, L., Cuamba, B., Feijó, J., & Zefanias Macome, A. (2021). Electricity access in Mozambique: A critical policy analysis of investment, service reliability and social sustainability. *Energy Research and Social Science*, 78(June). doi:10.1016/j.erss.2021.102123
- Sasitharan, S., Mishra, M. K., Kumar, B. K., & Jayashankar, V. (2008). Rating and design issues of DVR injection transformer. *Conference Proceedings - IEEE Applied Power Electronics Conference and Exposition - APEC*, 449–455. doi:10.1109/APEC.2008.4522760
- Sesay, S., Wara Tita, S., Mustapha, A. (2014). Effect of Dynamic Voltage Restorer in Compensating for Voltage Sag and Controlling Harmonics in a Power Distribution System using Fumman Industry as a Case Study The correlation between radon exhalation from refuse dumpsites and greenhouse gases found in . *International Journal of Engineering Innovation & Research*, 3(3), 2277–5668.
- Shah, M. S., Ullah, M. F., Nouman, D., Khan, M. A., Khan, T., & Waseem, M. (2024). A review on the state of the art of dynamic voltage restorer: topologies, operational modes, compensation methods, and control algorithms. *Engineering Research Express*, 6(1). doi:10.1088/2631-8695/ad2ccb
- Soomro, A. H., Larik, A. S., Sahito, A. A., Mahar, M. A., & Sohu, I. A. (2020). Simulation-based Analysis of a Dynamic Voltage Restorer under Different Voltage Sags with the Utilization of a PI Controller. *Engineering, Technology and Applied Science Research*, 10(4), 5889–5895. doi:10.48084/etasr.3524
- Tu, C., Guo, Q., Jiang, F., Wang, H., & Member, S. (2019). A Comprehensive Study to Mitigate Voltage Sags and Phase Jumps Using a Dynamic Voltage Restorer. *IEEE Journal of Emerging and Selected Topics in Power Electronics*, PP(c), 1. doi:10.1109/JESTPE.2019.2914308
- Zhan, C., Ramachandaramurthy, V. K., Arulampalam, A., Fitzner, C., Kromlidis, S., Barnes, M., & Jenkins, N. (2001). Dynamic voltage restorer based on voltage-space-vector PWM control. *IEEE Transactions on Industry Applications*, 37(6), 1855–1863. doi:10.1109/28.968201